

# Limits on the Stochastic Gravitational Wave Background and Prospects for Single Source Detection with GRACE Follow-On

M.P. Ross,\* C.A. Hagedorn, E.A. Shaw, A.L. Lockwood, B.M. Iritani, J.G. Lee, K. Venkateswara, and J. H. Gundlach  
*Center for Experimental Nuclear Physics and Astrophysics,  
 University of Washington, Seattle, Washington, 98195, USA*

With a reinterpretation of recent results, the GRACE Follow-On mission can be applied to gravitational wave astronomy. Existing GRACE Follow-On data constrain the stochastic gravitational wave background to  $\Omega_{GW} < 3.3 \times 10^7$  at 100 mHz. With a dedicated analysis, GRACE Follow-On may be able to detect the inspiral of local neutron star binaries, inspiral of subgalactic stellar-mass black hole binaries, or mergers of intermediate-mass black hole binaries within the Milky Way.

## I. INTRODUCTION

GRACE Follow-On (GRACE-FO) [1] is a satellite mission currently in Earth orbit studying the terrestrial gravitational field. We show that by interpreting recent results from this mission as strain, one can (1) constrain the gravitational wave background and (2) provide an opportunity for single-source gravitational wave (GW) searches.

Incoherent GW must be present throughout the universe at some amplitude. A broadband stochastic background is one of the few observable consequences of cosmic inflation [2] and a signature of proposed exotic phenomena such as cosmic strings [3]. Measurements of, and constraints on, such a background would yield insight into a wide range of phenomena, from inflationary models and predictions of string theory to populations of black holes and neutron stars. Existing limits on the stochastic background come from pulsar timing [4], satellite ranging [5, 6], torsion balances [7, 8], terrestrial interferometers [9], and geophysical observations [10–12].

The most prominent single-source GW are emitted either by binary systems or spinning asymmetric stars. While asymmetric stars emit GW with a quasi-stationary frequency, inspiraling binary systems radiate semi-monotone GW before a rapid merger and ring-down phase. The only direct observations of GW have been from the merger of black hole binaries and binary neutron stars [13–15] by the LIGO [16] and Virgo [17] observatories.

## II. STRAIN MEASUREMENTS

As a GW passes two inertial masses nominally separated by a distance  $x_0$  their relative displacement,  $x$ , is [18]:

$$x(t) = x_0 h_{xx} \cos(2\pi f t + \psi) \quad (1)$$

$$h_{xx} = h_+ (\cos^2 \theta \cos^2 \phi - \sin^2 \phi) + 2h_{\times} \cos \theta \sin \phi \cos \phi \quad (2)$$

where  $h_{+,\times}$  are the plus and cross-polarization components of the gravitational wave,  $\theta$  and  $\phi$  are the polar and azimuthal angles of the source,  $f$  is the wave frequency, and  $\psi$  is an arbitrary phase. Here, the plus and cross polarizations are defined in the source frame.

The GRACE-FO satellite mission has produced sensitive relative-displacement measurements of an inertial mass pair formed by its two satellites separated by  $x_0 = 220$  km. The published displacement spectrum [1] can be converted to strain via  $\tilde{h}_{xx}(f) = \tilde{x}(f)/x_0$ . The inferred strain-noise spectral density is shown in Figure 1. As noted in Ref. [1], the noise below 30 mHz may be significantly reduced by subtracting models of the terrestrial gravitational field.

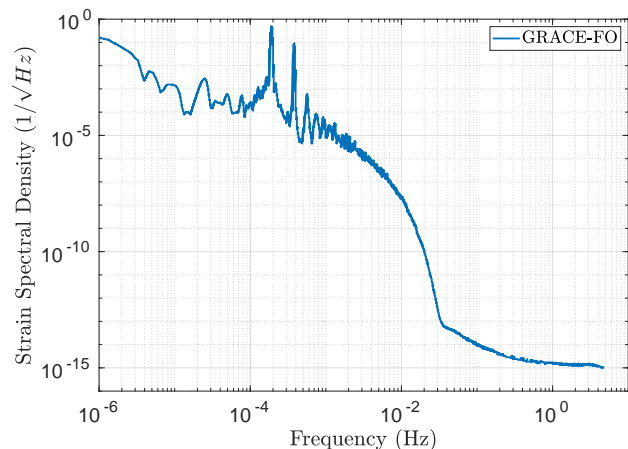


FIG. 1. Strain amplitude spectral density for the GRACE-FO mission. The increase in apparent noise below 30 mHz is due to terrestrial gravitational signals and not instrumental noise.

\* mpross2@uw.edu

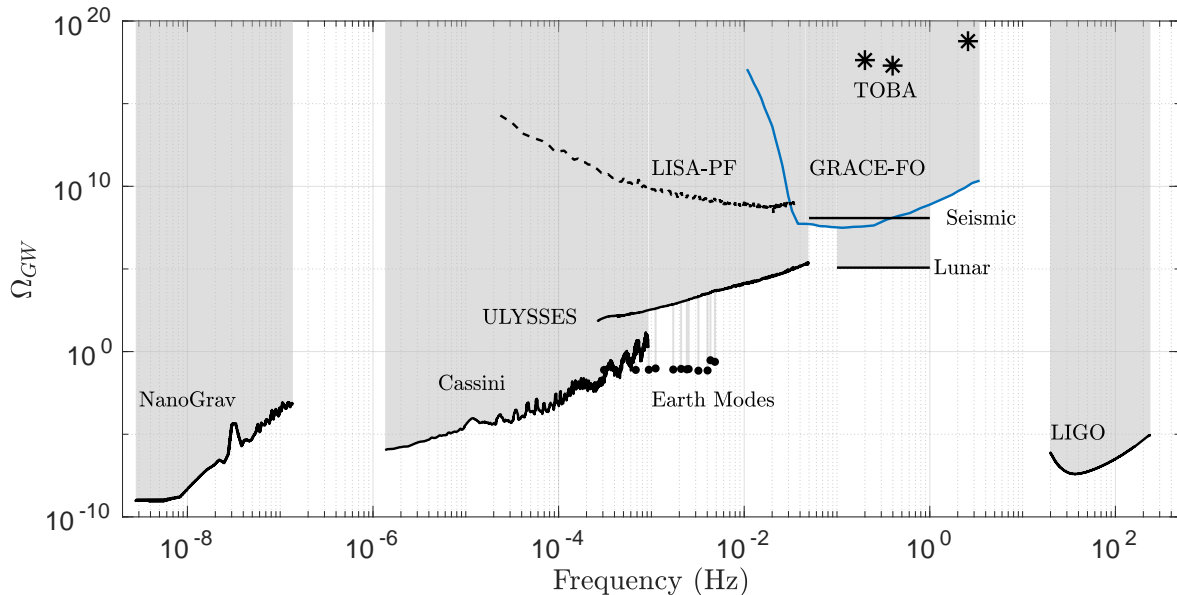


FIG. 2. Limits on the stochastic gravitational wave background set by GRACE-FO (blue) and LISA-PF (dashed). Analysis of LISA-PF is detailed in Appendix B. Additionally, limits set by NanoGrav [4], Cassini [5], ULYSSES [6], TOBA [7, 8], LIGO [9], observations of the earth’s normal modes [10], terrestrial seismic motion [11], and lunar seismic motion [12] are shown. Gray shading indicates regions excluded at 95% confidence.

### III. BACKGROUND CONSTRAINTS

Assuming an isotropic, unpolarized, stochastic gravitational wave background, this strain noise can be interpreted as limits on the cosmological energy density of gravitational waves,  $\Omega_{\text{GW}}$  [19], by integrating Equation 2 over incidence angle and polarization.

$$\Omega_{\text{GW}}(f) = \frac{f}{\rho_{\text{crit}}} \frac{d\rho_{\text{GW}}}{df} = \frac{32\pi^3}{3H_0^2} f^3 \frac{15}{4} \tilde{h}_{\text{meas}}(f)^2 \quad (3)$$

where  $\rho_{\text{crit}}$  is the critical energy density of the universe,  $\rho_{\text{GW}}$  is the energy density of gravitational waves,  $H_0$  is Hubble constant, and  $h_{\text{meas}}$  is the measured displacement interpreted as strain. A Hubble constant of  $H_0 = 70.3 \text{ km s}^{-1} \text{ Mpc}^{-1}$  was used [20]. The factor of 15/4 corrects for the polarization and angular sensitivity of the instruments in question, see Appendix A.

Confidence intervals were extracted from the GRACE-FO strain spectrum by separating the data into frequency bins which each encompassed 20 data points. Limits for each bin were set at the 95th percentile to yield the results shown in Figure 2. We anticipate that a dedicated analysis would improve these constraints further.

### IV. SINGLE-SOURCES

In addition to setting stochastic GW limits, the GRACE-FO mission may allow for gravitational wave

searches at frequencies between 30 mHz and 5 Hz. Both stellar-mass black hole binaries and neutron star binaries emit GW in the band of interest during their inspiral phase, while intermediate-mass black hole binaries would merge within the band.

Due to the orbit of the satellites, a GW seen by GRACE-FO would be modulated as the antenna pattern sweeps across the sky. This modulation can be approximated by rotating  $\phi$  at the orbit frequency,  $f_{\text{orb}} = 1/94.5 \text{ min}$  [1].

$$\phi(t) = 2\pi f_{\text{orb}} t + \phi_0 \quad (4)$$

Simulated antenna factors (the angular dependence of Equation 2) for GRACE-FO, at a collection of  $\theta$  values, are shown in Figure 3. For sources in-line with the orbital axis ( $\theta = 0$ ) the instrument’s polarization sensitivity is modulated, while for sources in the orbital plane ( $\theta = \pi/2$ ) the total observed power is modulated.

Detailed analysis of the orbit of the satellites and backgrounds due to the terrestrial gravitational field would be required for a definitive search. However, an estimate of the characteristic strain [21] sensitivity can be inferred from the strain spectral density. This is shown in Figure 4 along with a collection of known and speculative sources. The best characteristic strain sensitivity is  $2 \times 10^{-15}$  at 0.5 Hz.

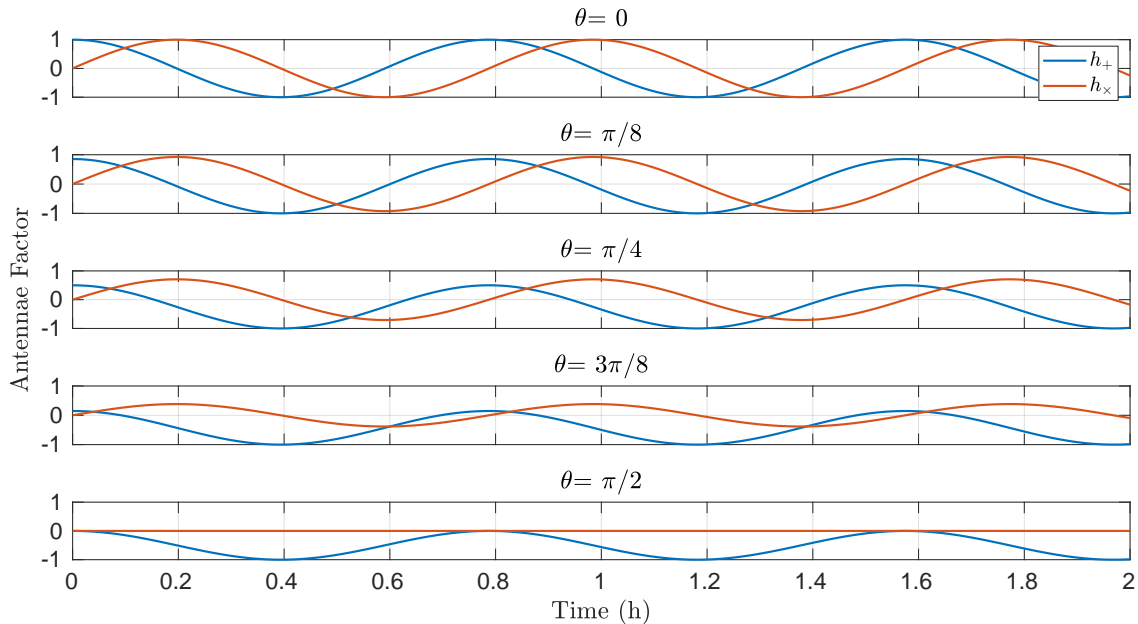


FIG. 3. Simulated antenna factors for  $h_+$  and  $h_\times$  where  $\theta$  is the polar angle of the source. For sources in-line with the satellite's orbital axis ( $\theta = 0$ ) the instrument's polarization sensitivity is modulated by the orbit, while for sources in the orbital plane ( $\theta = \pi/2$ ) the total observed power is modulated.

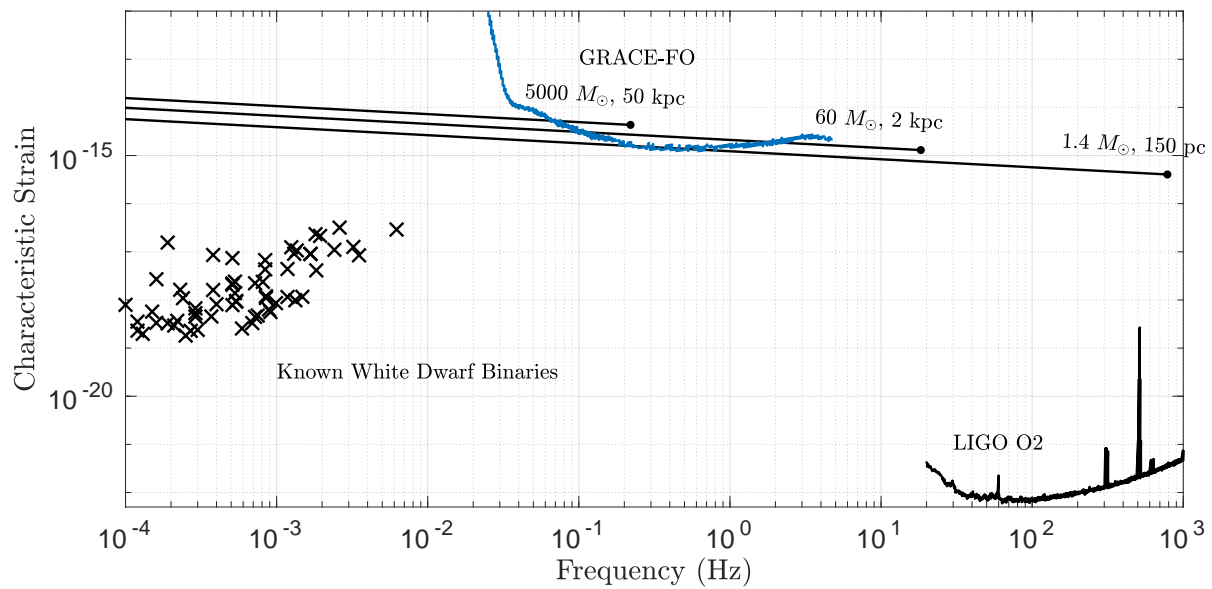


FIG. 4. Estimates of the characteristic strain sensitivity of GRACE-FO along with the expected strain from known white dwarf binaries [22–25] and a sensitivity curve for LIGO's second observing run [26]. Also shown are lines that correspond to the predicted characteristic strain of an equal component-mass  $1.4 M_\odot$  binary at 150 pc, a  $60 M_\odot$  at 2 kpc, and a  $5000 M_\odot$  at 50 kpc [21]. The points at the end of each line note the merger frequency for the corresponding system. These approximations are only valid for the inspiral phase of binary evolution.

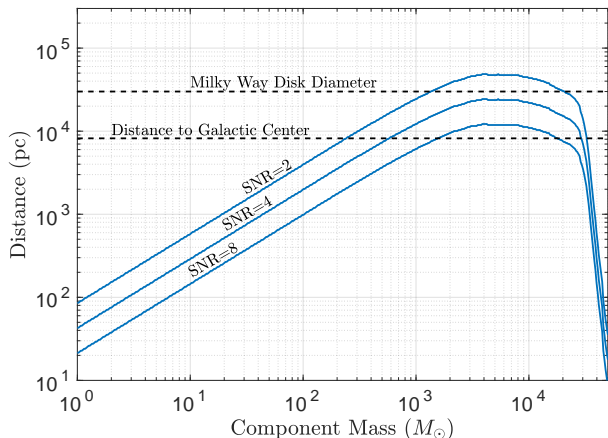


FIG. 5. Maximum detectable distance for equal component-mass binaries with SNR thresholds of 2, 4, and 8. For systems with component-mass of 2000-10000  $M_{\odot}$  the detection volume encompasses most of the Milky Way.

The characteristic strain allows for the estimation of the signal-to-noise ratio (SNR) of an optimal search for a given source [21]. Figure 5 shows the estimated maximum detectable distance for a given equal component-mass system with a select SNR threshold.

The detection range peaks at component-masses of 2000-10000  $M_{\odot}$  with a volume encompassing most of the Milky Way. Above 10000  $M_{\odot}$ , terrestrial gravitational

signals severely limit detection capability while below  $\sim 100 M_{\odot}$  the decreased emission does not provide an appreciable detection volume.

## V. CONCLUSION

Existing GRACE Follow-On data constrain the stochastic gravitational wave background to levels of  $\Omega_{GW} < 3.3 \times 10^{-7}$  at 100 mHz. These constraints are many orders of magnitude from expected sources [2], yet provide an independent set of limits in a frequency range where existing limits are sparse.

With a dedicated analysis, GRACE-FO is capable of single-source GW searches. Promising target systems include the inspiral of local neutron star binaries or sub-galactic stellar-mass black hole binaries, and the mergers of intermediate-mass black hole binaries within the Milky Way.

Although the application of this mission to gravitational wave astronomy will be supplanted by the launch of LISA [27], GRACE-FO has the capability to yield opportunistic insight into the local universe.

## ACKNOWLEDGMENTS

The authors would like to thank Eric Adelberger for his invaluable input and the anonymous referees for their insightful suggestions. This work was supported by funding from the NSF under Awards PHY-1607385, PHY-1607391, PHY-1912380 and PHY-1912514.

- 
- [1] Klaus Abich et al. In-orbit performance of the GRACE Follow-on laser ranging interferometer. *Phys. Rev. Lett.*, 123:031101, Jul 2019. doi: 10.1103/PhysRevLett.123.031101. URL <https://link.aps.org/doi/10.1103/PhysRevLett.123.031101>.
- [2] Richard Easther and Eugene A Lim. Stochastic gravitational wave production after inflation. *Journal of Cosmology and Astroparticle Physics*, 2006(04):010–010, Apr 2006. doi:10.1088/1475-7516/2006/04/010. URL <https://doi.org/10.1088/1475-7516/2006/04/010>.
- [3] Thibault Damour and Alexander Vilenkin. Gravitational radiation from cosmic (super)strings: Bursts, stochastic background, and observational windows. *Phys. Rev. D*, 71:063510, Mar 2005. doi:10.1103/PhysRevD.71.063510. URL <https://link.aps.org/doi/10.1103/PhysRevD.71.063510>.
- [4] Zaven Arzumian, Adam Brazier, Sarah Burke-Spolaor, Sydney Chamberlin, Shami Chatterjee, Brian Christy, James M. Cordes, Neil J. Cornish, Fronefield Crawford, H. Thankful Cromartie, Kathryn Crowder, Megan E. DeCesar, Paul B. Demorest, Timothy Dolch, Justin A. Ellis, Robert D. Ferdman, Elizabeth C. Ferrara, Emmanuel Fonseca, Nathan Garver-Daniels, Peter A. Gentile, Daniel Halmrast, E. A. Huerta, Fredrick A. Jenet, Cody Jessup, Glenn Jones, Megan L. Jones, David L. Kaplan, Michael T. Lam, T. Joseph W. Lazio, Lina Levin, Andrea Lommen, Duncan R. Lorimer, Jing Luo, Ryan S. Lynch, Dustin Madison, Allison M. Matthews, Maura A. McLaughlin, Sean T. McWilliams, Chiara Mingarelli, Cherry Ng, David J. Nice, Timothy T. Pennucci, Scott M. Ransom, Paul S. Ray, Xavier Siemens, Joseph Simon, Renée Spiewak, Ingrid H. Stairs, Daniel R. Stinebring, Kevin Stovall, Joseph K. Swiggum, Stephen R. Taylor, Michele Vallisneri, Rutger van Haasteren, Sarah J. Vigeland, and Weiwei Zhu. The NANOGrav 11-year data set: High-precision timing of 45 millisecond pulsars. *The Astrophysical Journal Supplement Series*, 235(2):37, Apr 2018. doi: 10.3847/1538-4365/aab5b0. URL <https://doi.org/10.3847/1538-4365/aab5b0>.
- [5] J. W. Armstrong, L. Iess, P. Tortora, and B. Bertotti. Stochastic gravitational wave background: Upper limits in the  $10^{-6}$  to  $10^{-3}$  Hz band. *The Astrophysical Journal*, 599(2):806–813, Dec 2003. doi:10.1086/379505. URL <https://doi.org/10.1086/379505>.
- [6] B. Bertotti, R. Ambrosini, J. W. Armstrong, S. W. Asmar, G. Comoretto, G. Giampieri, L. Iess, Y. Koyama, A. Messeri, A. Vecchio, and H. D. Wahlquist. Search for gravitational wave trains with the spacecraft ULYSSES. *AAP*, 296:13, Apr 1995.

- [7] Koji Ishidoshiro, Masaki Ando, Akiteru Takamori, Hirota Takahashi, Kenshi Okada, Nobuyuki Matsumoto, Wataru Kokuyama, Nobuyuki Kanda, Yoichi Aso, and Kimio Tsubono. Upper limit on gravitational wave backgrounds at 0.2 Hz with a torsion-bar antenna. *Phys. Rev. Lett.*, 106:161101, Apr 2011. doi:10.1103/PhysRevLett.106.161101. URL <https://link.aps.org/doi/10.1103/PhysRevLett.106.161101>.
- [8] Ayaka Shoda, Yuya Kuwahara, Masaki Ando, Kazunari Eda, Kodai Tejima, Yoichi Aso, and Yousuke Itoh. Ground-based low-frequency gravitational-wave detector with multiple outputs. *Phys. Rev. D*, 95:082004, Apr 2017. doi:10.1103/PhysRevD.95.082004. URL <https://link.aps.org/doi/10.1103/PhysRevD.95.082004>.
- [9] B. P. Abbott et al. Search for the isotropic stochastic background using data from Advanced LIGO's second observing run. *Phys. Rev. D*, 100:061101, Sep 2019. doi:10.1103/PhysRevD.100.061101. URL <https://link.aps.org/doi/10.1103/PhysRevD.100.061101>.
- [10] Michael Coughlin and Jan Harms. Constraining the gravitational wave energy density of the universe using earth's ring. *Phys. Rev. D*, 90:042005, Aug 2014. doi:10.1103/PhysRevD.90.042005. URL <https://link.aps.org/doi/10.1103/PhysRevD.90.042005>.
- [11] Michael Coughlin and Jan Harms. Upper limit on a stochastic background of gravitational waves from seismic measurements in the range 0.05–1 Hz. *Phys. Rev. Lett.*, 112:101102, Mar 2014. doi:10.1103/PhysRevLett.112.101102. URL <https://link.aps.org/doi/10.1103/PhysRevLett.112.101102>.
- [12] Michael Coughlin and Jan Harms. Constraining the gravitational-wave energy density of the universe in the range 0.1 Hz to 1 Hz using the Apollo Seismic Array. *Phys. Rev. D*, 90:102001, Nov 2014. doi:10.1103/PhysRevD.90.102001. URL <https://link.aps.org/doi/10.1103/PhysRevD.90.102001>.
- [13] B. P. Abbott et al. GWTC-1: A gravitational-wave transient catalog of compact binary mergers observed by LIGO and Virgo during the first and second observing runs. *Phys. Rev. X*, 9:031040, Sep 2019. doi:10.1103/PhysRevX.9.031040. URL <https://link.aps.org/doi/10.1103/PhysRevX.9.031040>.
- [14] BP Abbott et al. GW190425: Observation of a compact binary coalescence with total mass  $\sim 3.4 M_{\odot}$ . *arXiv preprint arXiv:2001.01761*, 2020.
- [15] The LIGO Scientific Collaboration and the Virgo Collaboration. GW190412: Observation of a binary-black-hole coalescence with asymmetric masses, 2020.
- [16] J Aasi et al. Advanced LIGO. *Classical and Quantum Gravity*, 32(7):074001, Mar 2015. doi:10.1088/0264-9381/32/7/074001. URL <https://doi.org/10.1088/0264-9381/32/7/074001>.
- [17] F Acernese et al. Advanced Virgo: a second-generation interferometric gravitational wave detector. *Classical and Quantum Gravity*, 32(2):024001, Dec 2014. doi:10.1088/0264-9381/32/2/024001. URL <https://doi.org/10.1088/0264-9381/32/2/024001>.
- [18] Michele Maggiore. *Gravitational waves: Volume 1: Theory and experiments*, volume 1. Oxford university press, 2008.
- [19] Bruce Allen and Joseph D. Romano. Detecting a stochastic background of gravitational radiation: Signal processing strategies and sensitivities. *Phys. Rev. D*, 59:102001, Mar 1999. doi:10.1103/PhysRevD.59.102001. URL <https://link.aps.org/doi/10.1103/PhysRevD.59.102001>.
- [20] K. Hotokezaka, E. Nakar, O. Gottlieb, S. Nissanke, K. Masuda, G. Hallinan, K. P. Mooley, and A. T. Deller. A Hubble constant measurement from superluminal motion of the jet in GW170817. *Nature Astronomy*, 3:940–944, Jul 2019. doi:10.1038/s41550-019-0820-1.
- [21] C J Moore, R H Cole, and C P L Berry. Gravitational-wave sensitivity curves. *Classical and Quantum Gravity*, 32(1):015014, Dec 2014. doi:10.1088/0264-9381/32/1/015014. URL <https://doi.org/10.1088/0264-9381/32/1/015014>.
- [22] Valeriya Korol, Elena M. Rossi, Paul J. Groot, Gijs Nelemans, Silvia Toonen, and Anthony G. A. Brown. Prospects for detection of detached double white dwarf binaries with Gaia, LSST and LISA. *Monthly Notices of the Royal Astronomical Society*, 470(2):1894–1910, 05 2017. ISSN 0035-8711. doi:10.1093/mnras/stx1285. URL <https://doi.org/10.1093/mnras/stx1285>.
- [23] Kevin B. Burdge, Jim Fuller, E. Sterl Phinney, Jan van Roestel, Antonio Claret, Elena Cukanovaite, Nicola Pietro Gentile Fusillo, Michael W. Coughlin, David L. Kaplan, Thomas Kupfer, Pier-Emmanuel Tremblay, Richard G. Dekany, Dmitry A. Duev, Michael Feeney, Reed Riddle, S. R. Kulkarni, and Thomas A. Prince. Orbital decay in a 20 minute orbital period detached binary with a hydrogen-poor low-mass white dwarf. *The Astrophysical Journal*, 886(1):L12, nov 2019. doi:10.3847/2041-8213/ab53e5. URL <https://doi.org/10.3847/2041-8213/ab53e5>.
- [24] J. J. Hermes, Mukremin Kilic, Warren R. Brown, D. E. Winget, Carlos Allende Prieto, A. Gianninas, Anjum S. Mukadam, Antonio Cabrera-Lavers, and Scott J. Kenyon. Rapid orbital decay in the 12.75-minute binary white dwarf J0651+2844. *The Astrophysical Journal*, 757(2):L21, sep 2012. doi:10.1088/2041-8205/757/2/L21. URL <https://doi.org/10.1088/2041-8205/757/2/L21>.
- [25] Kevin B Burdge, Michael W Coughlin, Jim Fuller, Thomas Kupfer, Eric C Bellm, Lars Bildsten, Matthew J Graham, David L Kaplan, Jan Van Roestel, Richard G Dekany, et al. General relativistic orbital decay in a seven-minute-orbital-period eclipsing binary system. *Nature*, 571(7766):528–531, 2019.
- [26] J. C. Driggers et al. Improving astrophysical parameter estimation via offline noise subtraction for Advanced LIGO. *Phys. Rev. D*, 99:042001, Feb 2019. doi:10.1103/PhysRevD.99.042001. URL <https://link.aps.org/doi/10.1103/PhysRevD.99.042001>.
- [27] Karsten Danzmann and the LISA study team. LISA: laser interferometer space antenna for gravitational wave measurements. *Classical and Quantum Gravity*, 13(11A):A247–A250, Nov 1996. doi:10.1088/0264-9381/13/11a/033. URL <https://doi.org/10.1088/0264-9381/13/11a/033>.
- [28] M. Armano et al. Beyond the required LISA free-fall performance: New LISA Pathfinder results down to 20  $\mu$ Hz. *Phys. Rev. Lett.*, 120:061101, Feb 2018. doi:10.1103/PhysRevLett.120.061101. URL <https://link.aps.org/doi/10.1103/PhysRevLett.120.061101>.

## VI. APPENDIX A

The strain along a single axis caused by a GW is [18]:

$$h_{xx} = h_+ (\cos^2 \theta \cos^2 \phi - \sin^2 \phi) + 2h_\times \cos \theta \sin \phi \cos \phi \quad (5)$$

where  $h_{xx}$  is the strain along the x-axis,  $h_{+,\times}$  are the strain amplitudes respectively in the plus and cross polarization, and  $\theta$  and  $\phi$  are the polar and azimuth angles, respectively.

Assuming isotropic emission, the fraction of incident power that is captured by a single-axis instrument can be found by:

$$\tilde{h}_{\text{meas}}^2(f) = \frac{1}{4\pi} \int \tilde{h}_{xx}^2(f) d\Omega \quad (6)$$

$$\begin{aligned} &= \frac{1}{4\pi} \int d\Omega [\tilde{h}_+^2(f) (\cos^2 \theta \cos^2 \phi - \sin^2 \phi)^2 \\ &\quad + 4\tilde{h}_\times^2(f) (\cos \theta \sin \phi \cos \phi)^2 \\ &\quad + 2\tilde{h}_+(f) \tilde{h}_\times(f) (\cos^2 \theta \cos^2 \phi - \sin^2 \phi) \\ &\quad \quad \times \cos \theta \sin \phi \cos \phi] \end{aligned} \quad (7)$$

$$= \frac{1}{4\pi} \left( \tilde{h}_+^2(f) \frac{22\pi}{15} + 4\tilde{h}_\times^2(f) \frac{\pi}{6} \right) \quad (8)$$

Further assuming an unpolarized background, the polarization can be averaged to yield:

$$\tilde{h}_+^2(f) = \tilde{h}_\times^2(f) = \frac{1}{2} \tilde{h}^2(f) \quad (9)$$

$$\tilde{h}_{\text{meas}}^2(f) = \frac{1}{8\pi} \tilde{h}^2(f) \left( \frac{22\pi}{15} + \frac{2\pi}{3} \right) \quad (10)$$

$$\tilde{h}_{\text{meas}}^2(f) = \frac{4}{15} \tilde{h}^2(f) \quad (11)$$

## VII. APPENDIX B

The technique used with GRACE-FO can also be applied to LISA Pathfinder (LISA-PF) [28] which was flown to demonstrate the drag-free technology needed for the future LISA mission [27]. For LISA-PF the mass-pair is formed by the proof masses, separated by  $x_0 = 376$  mm. LISA-PF has published an acceleration noise spectrum which can be converted to strain via  $\tilde{h}_{xx}(f) = -\frac{1}{x_0 \omega^2} \tilde{\ddot{x}}(f)$ . The corresponding strain spectral density is shown in Figure 6. This measurement can constrain the stochastic gravitational wave background to  $\Omega_{\text{GW}} < 6.5 \times 10^8$  at 10 mHz as seen in Figure 2.

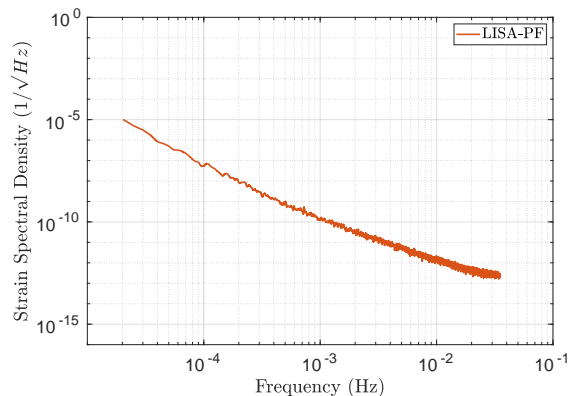


FIG. 6. Strain amplitude spectral density for LISA-PF.